MODELING THE THERMAL AND CHEMICAL EVOLUTION OF THE MARTIAN LITHOSPHERE THROUGH TIME. F. C. McGroarty[1], M. S. Duncan[1], and M. B. Weller[2], [1]Virginia Tech, 4044 Derring Hall, Virginia Tech, 926 West Campus Dr., Blacksburg, VA, USA (fcm@vt.edu, msd19@vt.edu), [2]Brown University, 324 Brook St., Providence, RI, USA (mbweller@brown.edu).

Introduction: To date, there are few constraints on the thermal evolution of Mars. Existing constraints arise from orbital and lander/rover observations of the surface and from meteorites. These indicate a crustal age range from the ~4 Byr old highlands to the <1 Myr old Olympus Mons lava flows [1-3]. The presence of recent lava flows indicates that the martian interior has been conducive to melting through its history. From gravity measurements and derived models, the crust is inferred to have a thickness of ~50 km and be composed of basaltic material [4,5].

Previous estimates of martian thermal history were derived from a combination of meteorites and surface basalts [6]. These showed a general trend of cooling from an average mantle potential temperature of 1450°C ~4 Ga, to 1345°C today. There are also constraints on the abundances of the Heat Producing Elements (HPE) in the current crust [4] and mantle [9], and models that calculated surface heat fluxes. Additionally, there are data from melting experiments from which the mineral/melt partitioning behavior of oxides were measured over a range of pressures and temperatures [7,8]. We will be using these parameters to calculate areotherms and crustal structures for the martian crust over the past 4 Gyr.

Methods: In order to constrain the planetary-scale thermal evolution at the crustal-scale geochemical level, we used a combination of observed parameters (above) and geochemical geodynamic models.

Geochemical: We modeled crustal evolution by first calculating a range of modern day areotherms. Using the thickness, heat production, heat flow, thermal conductivity, and density for the present-day crust, we constructed the areotherms using [9-14]:

$$T(z) = T_0 + q_i \Delta z_i / k_i - A_i \Delta z_i^2 / 2k_i$$

where T_0 is the surface temperature (K), q_i is the heat flow (W/m^2), z_i is the depth (m), k_i is the thermal conductivity (W/mK) [9,12], and A_i is the volumetric radiogenic heat production of layer i (W/m^3).

We began with a reference case of a homogenous HPE distribution within the crust [4] and an undepleted lithospheric mantle [5], using the average thickness of 50 km today, and average modern heat flow of 25 mW/m^2 based on previously calculated values [e.g., 12]. As heat production in the crust is related to the abundance of HPEs, which changes over time as a function of radioactive decay, we calculated areotherms through time. From this, we inferred how the crust evolved over time. The areotherms were used in conjunction with previously calculated adiabatic profiles [6] and a mantle solidus [16] to determine melt fraction (F) [17], and therefore potential crustal compositions, through time.

We used least squares regression to fit a melting model as a function of P and F to existing experimental data [7,8], producing a set of equations that calculate the composition of oxides within the melt based on the relationship between melt percent and pressure [e.g., 18]. These equations follow the form of polynomials for the oxides SiO_2, Al_2O_3, Cr_2O_3, FeO, MnO, MgO, and CaO. They follow the form of exponentials for the oxides Na_2O and K_2O. We determined the proper form of the equation by fitting the model to the experimental data in order to find the best fit. We calculated coefficients by set pressure ranges to determine the equation by which the experimental compositions are related to melt percent and pressure; we then parameterized said coefficients as a function of pressure in order to set one equation per oxide. We used this melt model to calculate the melt composition over time, using the P and F values derived from our geochemical (fig. 1) and geodynamic (fig. 2) areotherm models. At each billion year increment, F was calculated using the constraints in the areotherm and method in [18]. The melt composition was then calculated for the F based on our melt model. The trends in the melt model show the changes in the various oxides from the initial, presumed homogenous mantle composition through the melting and depletion to the composition of the crust and depleted mantle lithosphere observed today (fig.3).

We then calculated the mineral modes in the crust and mantle lithosphere using a NORMs calculator for the crust and Perple_X [19] for the mantle lithosphere. These mineral modes will be used to calculate the densities and seismic properties of the lithosphere through time.

Geodynamic: We used CitcomS [20] to calculate average mantle areotherms. We used fully spherical 3D models, as opposed to 1D models in the geochemical calculations. These profiles employed a constant boundary temperature at the surface (T = -53 ºC) and at the CMB (T = 1547 ºC); with an adiabat of 0.18 ºC/km [16]) and a Rayleigh number of 3x10^6. They considered variable internal heating rates and core fractions of 0.45 (S-bearing) and 0.4 (S-poor) of the total planet radius. From these profiles, we determined average surface heat flux and F through time.

Preliminary Results: Our initial areotherms were calculated using a surface heat flux of 25 mW/m^2 for the present day and 50 mW/m^2 for 4 Ga [14, 21], values for *A* based on the present day HPE concentrations [4,9] and those calculated 4 Ga, and a crustal thickness of 50 km for the present and ~20 km for 4 Ga (Fig. 1). Based on these results, there is an observable cooling of the crust as the temperature decreases at given pressure, correlated with dwindling of radiogenic heat production a general thickening of the lithosphere. The comparison between the present day and 4 Ga shows a significantly hotter lithosphere in the past,~1700 K at the base of lithosphere, which cools to~ 1610 K at the base of the lithosphere in the present day.

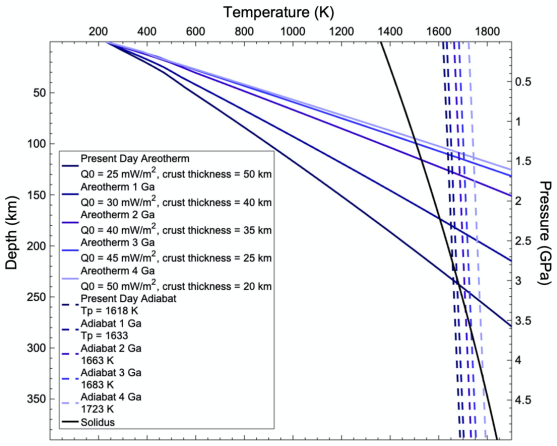

Figure 1. Global averaged geochemically-derived areotherms (solid lines) for the modern day (dark blue) [9-13] through 4 Ga (light blue). Also shown are the mantle adiabats (dashed lines) in the same respective colors and solidus (black). The areotherms show a trend of cooling from 4 Ga to the present day, combined with subsequent loss of melt production.

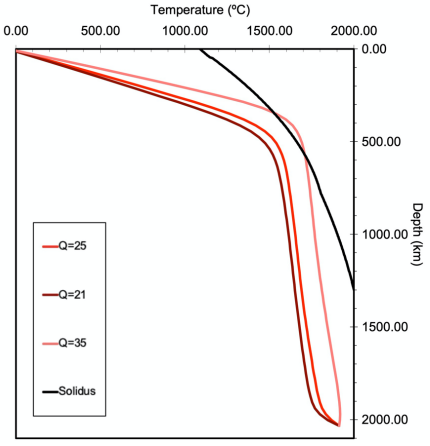

Figure 2. Global average areotherms from CitcomS at a fixed core fraction of 0.40 and *Q* values decreasing from 35 to 21, showing evolution through time (~2.8 Ga to the present). Also shown is the solidus (black line).

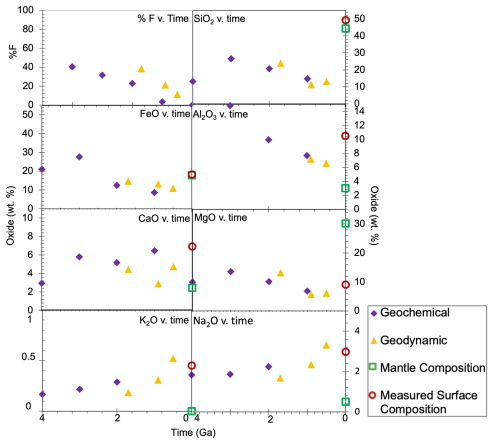

Figure 3. Melt model results for initial areotherms calculated from geochemical assumptions only (Fig. 1, purple diamonds) and calculated from geodynamic assumptions only (Fig. 2, yellow triangles). Overall, there is decrease in melt production and change in melt composition over time. Also shown are the present-day observed surface composition [4] (red circle) and the mantle composition [9] (green box)

Conclusions: This project will provide further insight into the thermal and cooling history of Mars. The model will provide a possible history of the global average chemical and mineralogical composition of the lithosphere. Knowing the mineralogical composition of the lithosphere will also provide constraints on the global average density and seismic properties of the lithosphere. The properties calculated in the present day will be compared to properties observed by NASA's InSight lander.

References: [1] Grott et al. (2013) *Space Sci. Rev.*, *174*, 49–111. [2] Hartmann. (2005) *Icarus*, *174*, 294–320. [3] Werner. (2009) *Icarus*, *201*, 44–68. [4] Taylor and McLennan. (2009) *Planetary Crusts*, 141–180. [5] Neumann et al. (2004) *JGR.* 109. [6] Filiberto. (2017) *CG*, *466*, 1–14. [7] Collinet et al. (2015) *EPSL*, 84–93. [8] Matsukage et al. (2013) *J. Min. Pet. Sci.*, 201–214. [9] Dreibus and Wänke. (1985) *Meteor*, *20*, 367–381. [10] Chapman. (1986) *Geol. Soc. Spec. Publ.*, 63–70. [11] Pollack and Chapman. (1977) *Tectonophysics*, 279–296. [12] Rudnick et al. (1998) *Geol., 145*, 395–411. [13] Schatz and Simmons. (1972) *JGR, 77*, 6966–6983. [14] Plesa et al. (2016) *JGR, 121*, 2386–2403. [16] Duncan et al. (2018) *GRL, 45*, 10211–10220. [17] Duncan et al., (2017) *EPSL*, 115-128 [18] Kiefer. (2003) *MaPS*, *38*, 1815–1832. [19] Holland and Powell. (1998) *J. Metamorph. Geol., 16*, 309–343. [20] Zhong et al. (2000) *JGR*, *105*, 11063–11082. [21] Parro, L.M., et al. (2017) *Sci. Rep.,* 45629